Fermi National Accelerator Laboratory

FERMILAB-Pub-93/065-E

E665

Measurement of the Ratio σ_n/σ_p in Inelastic Muon-nucleon Scattering at very low x and Q^2

M.R. Adams et al
the E665 Collaboration

Fermi National Accelerator Laboratory
P.O. Box 500, Batavia, Illinois 60510

March 1993

Submitted to *Physics Letters B*

Disclaimer

Measurement of the ratio σ_n/σ_p in inelastic muon–nucleon scattering at very low x and Q^2

THE FERMILAB E665 COLLABORATION

Fermi National Accelerator Laboratory
P.O. Box 500, Batavia, Illinois, 60510

March 18, 1993

Abstract

We present results on the cross-section ratio for inelastic muon scattering on neutrons and protons as a function of Bjorken x. The data extend to x values two orders of magnitude smaller than in previous measurements, down to 2×10^{-5}, for $Q^2 > 0.01$ GeV^2. The ratio is consistent with unity throughout this new range.

Submitted to Physics Letters B

THE FERMILAB E665 COLLABORATION

M.R. Adams[a], S.Aïd[b,1], P.L. Anthony[c,2], M.D. Baker[c], J. Bartlett[d], A.A. Bhatti[e,3], H.M. Braun[f], W. Busza[c], T.J. Carroll[a], J.M. Conrad[g], G. Coutrakon[d,4], R. Davisson[e], I. Derado[h], S.K. Dhawan[i], W. Dougherty[e], T. Dreyer[j], K. Dziunikowska[k], V. Eckardt[h], U. Ecker[f,1], M. Erdmann[j,5], A. Eskreys[l], J. Figiel[l], H.J. Gebauer[h], D.F. Geesaman[m], R. Gilman[m,6], M.C. Green[m,7], J. Haas[j], C. Halliwell[a], J. Hanlon[d], D. Hantke[h], V.W. Hughes[i], H.E. Jackson[m], D.E. Jaffe[a,8], G. Jancso[h], D.M. Jansen[e,9], S. Kaufman[m], R.D. Kennedy[n], T. Kirk[d,10], H.G. E. Kobrak[n], S. Krzywdzinski[d], S. Kunori[b], J.J. Lord[e], H.J. Lubatti[e], D. McLeod[a], S. Magill[a,10], P. Malecki[l], A. Manz[h], H. Melanson[d], D.G. Michael[g,11], W. Mohr[j], H.E. Montgomery[d], J.G. Morfin[d], R.B. Nickerson[g,12], S. O'Day[b,13], K. Olkiewicz[l], L. Osborne[c], V. Papavassiliou[i,10], B. Pawlik[l], F.M. Pipkin[g,14], E.J. Ramberg[b,13], A. Röser[f,15], J.J. Ryan[c], A. Salvarani[n,16], H. Schellman[o], M. Schmitt[g,17], N. Schmitz[h], K.P. Schüler[i,18], H.J. Seyerlein[h], A. Skuja[b], G.A. Snow[b], S. Söldner-Rembold[h,19], P.H. Steinberg[b,14], H.E. Stier[j,14], P. Stopa[l], R.A. Swanson[n], R. Talaga[b,10], S. Tentindo-Repond[m,20], H.-J. Trost[m,21], H. Venkataramania[i], M. Vidal[h], M. Wilhelm[j], J. Wilkes[e], Richard Wilson[g], W. Wittek[h], S.A. Wolbers[d], and T. Zhao[e]

[a] University of Illinois, Chicago, IL 60680 USA
[b] University of Maryland, College Park, MD 20742, USA
[c] Massachusetts Institute of Technology, Cambridge, MA 02139 USA
[d] Fermi National Accelerator Laboratory, Batavia, IL 60510, USA
[e] University of Washington, Seattle, WA 98195, USA
[f] University of Wuppertal, Wuppertal, Germany
[g] Harvard University, Cambridge, MA 62138, USA
[h] Max-Planck-Institut für Physik, Munich, Germany
[i] Yale University, New Haven, CT 06520, USA
[j] Albert-Ludwigs-Universität, W-7800 Freiburg, Germany
[k] Institute for Nuclear Physics, Academy of Mining and Metallurgy, Crakow, Poland
[l] Institute for Nuclear Physics, PL-31 342 Crakow, Poland
[m] Argonne National Laboratory, Argonne, IL 60439, USA
[n] University of California at San Diego, La Jolla, CA 92093, USA
[o] Northwestern University, Evanston, IL 60208, USA

Recently, there has been considerable interest in the very small x ($x < 10^{-2}$) behavior of the nucleon structure functions in inelastic lepton-nucleon scattering. Here x is the Bjorken scaling variable, $x = Q^2/2M\nu$, where $-Q^2$ is the invariant mass squared of the virtual photon that mediates the interaction, ν is the energy transfer (photon energy) in the laboratory frame, and M is the proton mass. Theoretical calculations based on Perturbative Quantum Chromodynamics (PQCD) make interesting predictions for the small-x range, where the parton densities are predicted to be very large[1, 2]. In current fixed-target experiments, this kinematic region can be accessed only at low Q^2 ($Q^2 < 1$ GeV^2), where PQCD is not applicable. It can however be studied using the concepts of Regge theory. Recent investigations[3, 4] give predictions for the structure functions of the nucleon at low x down to $Q^2 = 0$, while at higher Q^2 they reproduce fits of deep inelastic scattering data.

The latest precise NMC data[5] on the proton and neutron structure functions F_2^p and F_2^n cover the range $x > 0.006$, $Q^2 > 0.5$ GeV^2. The ratio F_2^n/F_2^p has been measured[6] down to $x = 0.002$, and is found to approach 1 at the lowest x values. Similarly, data[7] on the total absorption cross sections of real photons ($Q^2 = 0$) on H_2 and D_2 show that the proton and neutron cross sections differ by only a few percent in the range $\nu = 4 - 18$ GeV, approaching a common value at large ν. It is desirable to study the transition between these two regions, when $x \to 0$ while ν is large. This is the transition from hard to soft processes, from the large-Q^2 domain of PQCD to that of real photoproduction, as the mass of the virtual photon approaches zero.

Preliminary results on the ratio F_2^n/F_2^p from this experiment, covering the range $x > 10^{-3}$, can be found in [8]. In this paper, we present results on the ratio of inelastic cross sections σ_n/σ_p in muon scattering on neutrons and protons that include, for the first time, the range $2 \times 10^{-5} < x < 2 \times 10^{-3}$, with $Q^2 > 0.01$ GeV^2 and $\nu > 50$ GeV. This ratio is equal to the ratio F_2^n/F_2^p, under some assumptions. The single-photon-exchange cross section is given by

$$\frac{d^2\sigma}{dxdQ^2} = \frac{4\pi\alpha^2}{Q^4 x}\frac{E'}{E}[\cos^2\frac{\theta}{2} + 2\frac{1+\nu^2/Q^2}{1+R(x,Q^2)}\sin^2\frac{\theta}{2}]F_2(x,Q^2), \qquad (1)$$

where $E(E')$ is the energy of the incoming (outgoing) muon, θ is the scattering angle in the laboratory frame, α is the fine-structure constant, and $R = \sigma_L/\sigma_T$ is the ratio of the longitudinal and transverse total cross sections. Therefore, the cross-section ratio is equal to the F_2 ratio if R is the same for protons and neutrons, as suggested by an analysis[9] of data from SLAC at higher x and Q^2, and provided higher-order electromagnetic processes modify the single-photon-exchange cross sections for the two targets to the same extent.

Data were taken in the Fermilab muon beam using the E-665 double-dipole open-geometry magnetic spectrometer[10] during the 1987–88 fixed-target run. The relevant data for this analysis were obtained at 490 GeV mean beam energy on a 1.15 m-long cryogenic target, filled initially with liquid D_2 (density 0.16 g/cm^3, 0.15 radiation lengths), and then with liquid H_2 (0.07 g/cm^3, 0.13 radiation lengths). The Small-Angle Trigger (SAT)[10] triggered on the absence of a veto signal at the expected position of the unscattered beam. This was calculated by a hardware processor for each incoming beam track detected in a set of 7 scintillator planes. The acceptance of the trigger extended to scattering angles smaller than 0.1 mrad, inside the phase space of the unscattered beam.

The scattered muon was identified in the off-line analysis by its ability to penetrate a set of steel and concrete absorbers; its trajectory was reconstructed with proportional and drift chambers. An electromagnetic calorimeter was used to discriminate between electrons and hadrons and to detect neutral particles depositing electromagnetic energy.

Events were selected by requiring both the incoming and scattered muon to be fully reconstructed and fitted to a vertex within the fiducial volume of the target, with a χ^2 probability greater than 10^{-3}. The following kinematic cuts were applied to constrain the data sample away from regions where the resolution in the kinematic variables is poor, or the radiative corrections can be large: $E > 400$ GeV, $Q^2 > 0.01$ GeV^2, $x > 2 \times 10^{-5}$, $0.1 < y < 0.9$, $\nu > 50$ GeV, and $|\phi - \pi| > 0.2$. Here $y = \nu/E$ is the fractional energy transfer and ϕ is the azimuthal angle of the scattered muon around the incoming muon direction. This last cut eliminated events with the outgoing muon close to the horizontal (bending) plane, for which the vertex was poorly determined. The resolution in x is approximately constant at $\sim 16\%$ for $x > 10^{-3}$ but this value increases to about 60% at the lowest x.

In addition to the above cuts, two independent methods were employed to separate inelastic events from the large electromagnetic backgrounds, not related to the nucleon structure, that dominate the event samples at $x < 10^{-3}$. These backgrounds are due to elastic muon-electron (μe) scattering in the target, and to muon bremsstrahlung. The first appears as a peak in the x distribution centered at $x = m_e/M \approx 5 \times 10^{-4}$, where m_e is the electron mass, with a width consistent with the experimental resolution at this x value. The second background appears as events with large energy loss (ν), reconstructed with very small scattering angles, and therefore at very low x. Figure 1 shows the event distribution in x after the kinematic cuts (solid histogram), with the μe peak clearly visible.

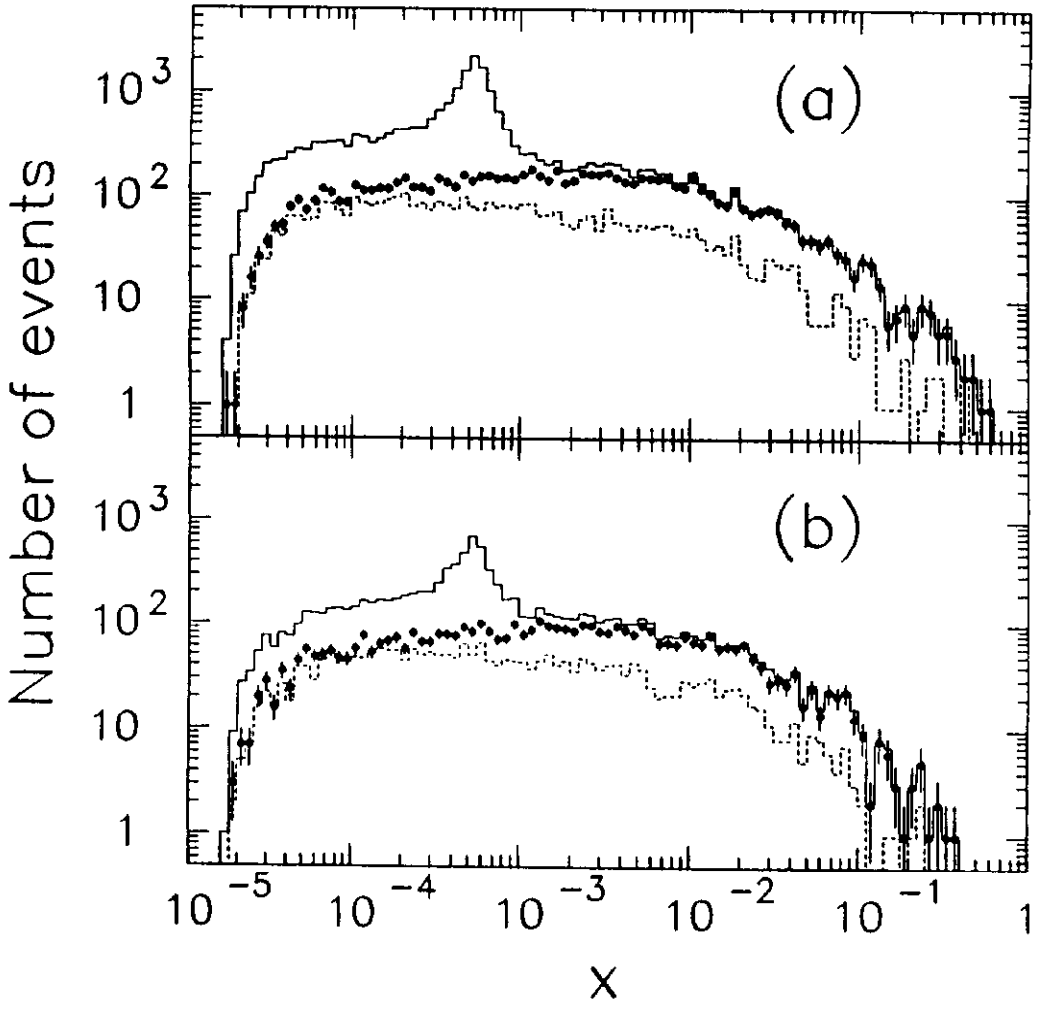

Figure 1. Event distribution vs. x from H_2 (a) and D_2 (b) after kinematic cuts only (solid line), kinematic and calorimeter cuts (black dots), and kinematic and multiplicity cuts (dotted line).

The two methods of background removal are similar to those used previously by this experiment in measuring the cross-section ratio for Xe and D_2 targets in the same kinematic range[11]. In the first method, referred to as "calorimeter cuts," electromagnetic events were rejected by selecting only those events for which the total electromagnetic energy $E_{\rm CAL}$ deposited in the calorimeter was less than 0.5ν, or for which the bremsstrahlung planarity $\mathcal{P}$ was greater than 10^{-5}. This last quantity is defined from the momentum vectors $\mathbf{p}$ and $\mathbf{p}'$ of the incoming and outgoing muons, and the vector $\mathbf{k}$ connecting the vertex to the largest energy cluster on the calorimeter, as

$$\mathcal{P} = \frac{|(\mathbf{p} \times \mathbf{p}') \cdot \mathbf{k}|}{|\mathbf{p}||\mathbf{p}'||\mathbf{k}|} = \sin\theta \sin\psi, \tag{2}$$

where ψ is the angle of $\mathbf{k}$ out of the scattering plane. Planar events have $\mathcal{P} = 0$. Bremsstrahlung photons tend to be in the scattering plane, whereas clusters from inelastic events need not be. Elastic μe events also appear at small values of $\mathcal{P}$.

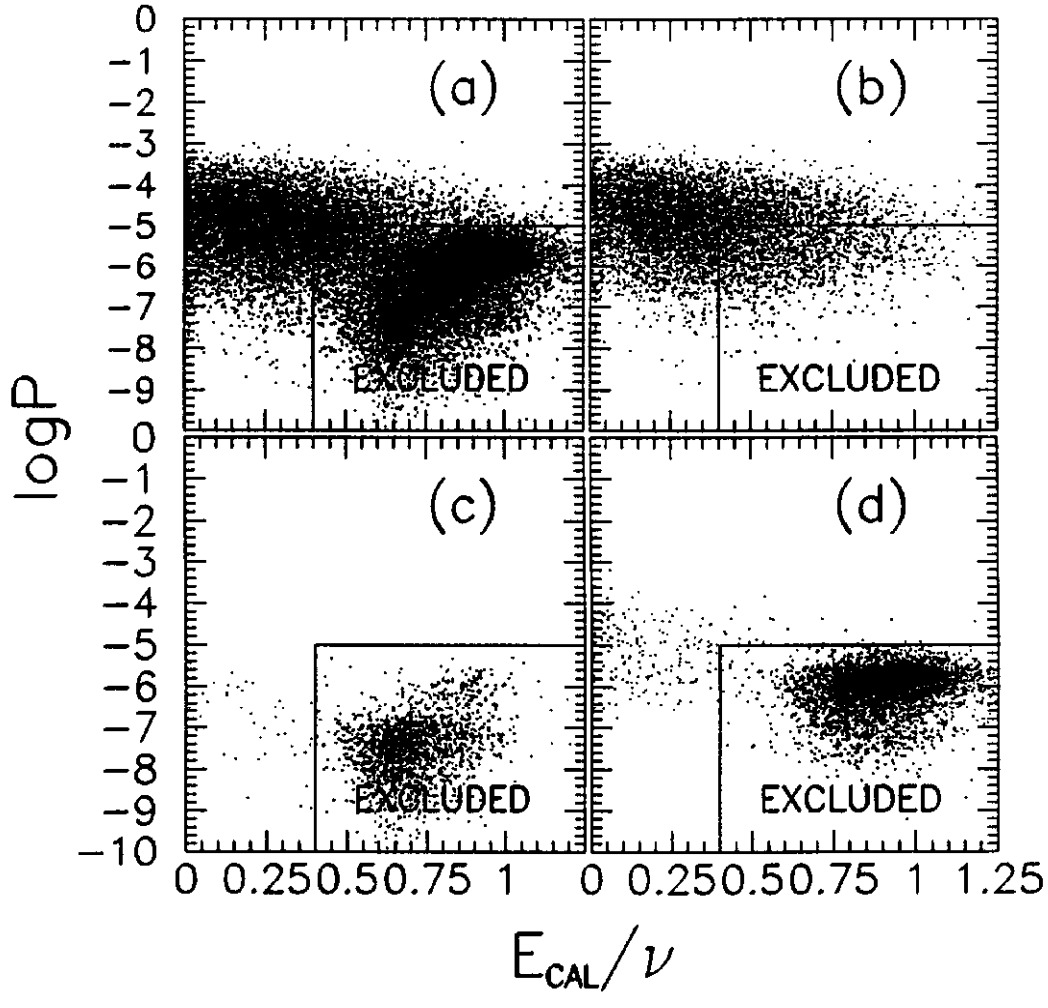

Figure 2. $\log \mathcal{P}$ vs. E_{CAL}/ν for all events (a), and for three different event types, inelastic (as defined by the multiplicity cuts), bremsstrahlung, and elastic μe (b–d), classified without use of the calorimeter. The area denoted as EXCLUDED is the region excluded by the calorimeter cuts.

The resulting distribution is shown in Figure 1 as black dots. Figure 2 shows the event distribution from both targets on the $\log \mathcal{P}$ vs. $E_{\rm CAL}/\nu$ plane for all events (a); inelastic events, as determined by the second method below (b); μ-bremsstrahlung events, *i.e.* events with $x < 10^{-4}$ and no additional tracks besides the scattered muon (c); and elastic μe events, identified as events with one muon and only one negative track in the final state, and kinematically consistent with μe scattering (d). A correction was applied to $E_{\rm CAL}$ for non-linearities and saturation effects in the

calorimeter response. The distributions from the two targets separately look very similar after the correction. The boxes show the regions excluded by the cuts. It can be seen that the cuts remove essentially all electromagnetic events of either type, while most of the inelastic events, as defined by the second method, are retained.

In the second method, referred to as "multiplicity cuts," inelastic events were explicitly selected by requiring at least two hadrons of the same sign to be associated with the event. Here a "hadron" was defined as any reconstructed track compatible with coming from the event vertex, other than the scattered muon or other muons. In general, only tracks going forward in the center-of-mass frame were within the spectrometer acceptance. In order to keep the two methods independent, no rejection of electrons by means of the calorimeter was performed. The same-sign requirement was imposed to avoid contamination from photons converting into e^+e^- pairs. The result is shown in Figure 1 as a dotted line. At low x, similar numbers of events are selected by the two methods. At higher x, however, the number of events selected by the second method is much smaller. This is due to smaller ν values resulting in lower charged multiplicities, which are further reduced by the smaller acceptance for low-momentum tracks by the forward spectrometer.

The ratio σ_n/σ_p was derived from the event yields from the H_2 and D_2 targets and the target densities and beam fluxes, assuming the deuteron cross section per nucleon to be $\sigma_d = (\sigma_p + \sigma_n)/2$. The ratio was corrected for events originating in the target vessel, as determined from an empty-target run, and for a 5% contamination of the D_2 target with HD molecules. No corrections were applied for Fermi motion, the effect of which is expected[12] to be negligible at $x < 0.6$, or for nuclear shadowing effects in the deuteron. Also, no radiative corrections were performed, other than the removal of the backgrounds described above. The remaining radiative corrections on the ratio are expected to be small, implying that the ratio of the single-photon-exchange cross sections should be approximately equal to the one presented here. This expectation is supported by a study in which the upper cut on y was varied in order to reduce further the influence of radiative effects; the results were essentially unchanged.

Figure 3 shows the ratio σ_n/σ_p as a function of x, as derived by the two methods. Only statistical errors are shown. The two methods give compatible results, within the statistical uncertainties, giving confidence that the electromagnetic backgrounds have been removed properly. In the following, the results from the first method will be used, because of the better statistics, especially at higher x.

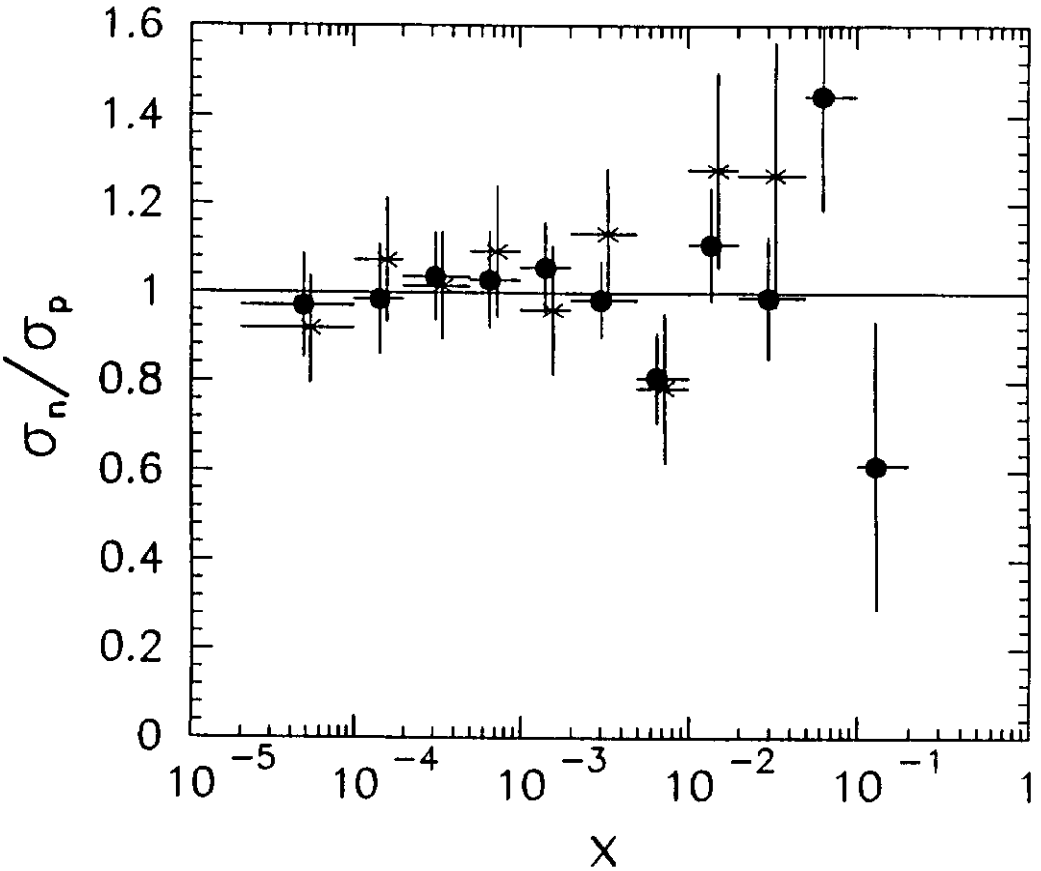

Figure 3. σ_n/σ_p versus x obtained with calorimeter (•) and multiplicity (×) cuts. The two sets of points are slightly displaced horizontally for clarity. The vertical error bars show the statistical errors, while the horizontal error bars show the extent of the x bins.

Systematic errors include a ±2% uncertainty on the relative beam fluxes and a ±3% uncertainty on the relative acceptance for the two data samples, which were taken in different running periods. These relative normalization uncertainties for the D_2 and H_2 runs result in a ±7% total normalization uncertainty on σ_n/σ_p. As a further check on the relative normalization, the cross-section ratio for elastic μe scattering from the D_2 and H_2 targets, which should be equal to 1, was measured to be 1.01 ± 0.03 (statistical error).

The calorimeter was cross-calibrated for the two data-taking periods using electrons from elastic μe events. The uncertainty in the subtraction of the electromagnetic backgrounds due to possible residual differences in the calorimeter response were included in the systematic error. This uncertainty is negligible for $x > 10^{-3}$.

Figure 4 and Table 1 show the ratio obtained with the calorimeter cuts with

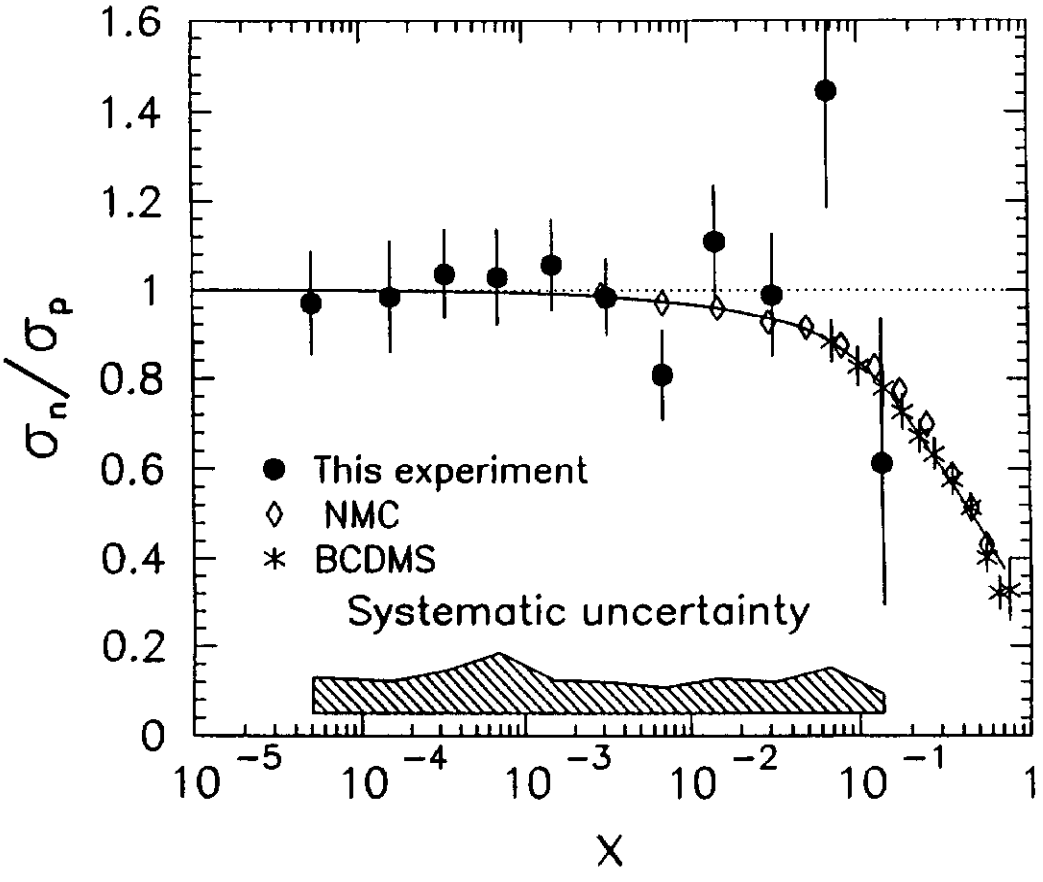

Figure 4. Results on σ_n/σ_p vs. x ($\bullet$) using the calorimeter method. The error bars show the statistical errors, while the shaded band shows the estimated systematic uncertainties. The curve is the prediction from [3]. Also shown are previous results on F_2^n/F_2^p from NMC[6] ($\diamond$) and BCDMS[13] ($\times$) (statistical errors only).

statistical and systematic errors. The mean value of the ratio in the range $2\times10^{-5} < x < 2\times10^{-3}$ is 1.02 ± 0.05(stat.)± 0.09(syst.). Table 1 also shows the ratio σ_d/σ_p with its statistical error. The invariant mass W of the hadronic final state of the data is always greater than 10 GeV, far above the resonance region, with an average varying from 25 GeV at the lowest x values to 12 GeV at the highest. Also shown in Figure 4 are the results for F_2^n/F_2^p from two previous high-statistics experiments, NMC[6] and BCDMS[13]. The curve is a prediction[3] based on the vector-meson dominance model.

The effect of nuclear shadowing on deuterium is at present unknown, as no experimental measurements exist. Different calculations predict an effect of up to 2%[14], or 4%[15], at some values of x and Q^2, but these calculations do not extend to the full kinematic range of this experiment. Shadowing would reduce the observed deuteron cross section compared to the one for free nucleons. If such an effect

Table 1: Results for σ_n/σ_p in x bins

lower x limit	upper x limit	$< x >$	$< Q^2 >$ (GeV^2)	σ_d/σ_p	stat. error	σ_n/σ_p	stat. error	syst. error
0.00002	0.0001	0.00005	0.03	0.99	0.06	0.97	0.12	0.08
0.0001	0.0002	0.00015	0.08	0.99	0.06	0.99	0.13	0.07
0.0002	0.0005	0.0003	0.16	1.02	0.05	1.04	0.10	0.10
0.0005	0.001	0.0007	0.3	1.02	0.05	1.03	0.11	0.13
0.001	0.002	0.0015	0.5	1.03	0.05	1.06	0.10	0.07
0.002	0.005	0.003	1.0	0.99	0.04	0.98	0.09	0.07
0.005	0.01	0.007	1.9	0.90	0.05	0.81	0.10	0.06
0.01	0.02	0.015	3.7	1.06	0.06	1.11	0.13	0.08
0.02	0.05	0.03	7.4	1.00	0.07	0.99	0.14	0.07
0.05	0.1	0.07	16.6	1.22	0.13	1.45	0.26	0.10
0.1	0.2	0.15	28.8	0.81	0.16	0.61	0.32	0.04

exists, the true values of σ_n/σ_p are higher than presented here, by twice the size of the shadowing effect.

The new results extend to x values two orders of magnitude lower than in previous measurements. The ratio is equal to 1, within errors, throughout this new range, consistent with the extrapolation of the NMC measurement. The validity of this extrapolation was crucial for the derivation[6] of the integral of the difference $F_2^p(x) - F_2^n(x)$ and the conclusion that the Gottfried sum rule[16] is violated. The present data bridge the gap between the high-x, high-Q^2 deep inelastic scattering data[6] and those from real photoproduction at lower photon energies[7].

The equality of the neutron and proton cross sections for $x \to 0$ is expected from Regge arguments[1, 3]. Our result is consistent with this expectation, provided any shadowing effects are small compared to the experimental uncertainties. Alternatively, if this equality is assumed to hold, then the above result suggests, within the precision of this experiment, the absence of significant nuclear shadowing effects in the deuteron.

We wish to thank all those personnel, both at Fermilab and at the participating institutions, who have contributed to the success of this experiment. This work was performed at the Fermi National Accelerator Laboratory, which is operated by Universities Research Association, Inc., under contract DE-AC02-76CHO3000 with the U.S. Department of Energy. The work of the University of California, San Diego was

supported in part by the National Science Foundation, contract numbers PHY82-05900, PHY85-11584, and PHY88-10221; the University of Illinois at Chicago by NSF contract PHY88-11164; and the University of Washington by NSF contract numbers PHY83-13347 and PHY86-13003. The University of Washington was also supported by the U.S. Department of Energy. The work of Argonne National Laboratory was supported by the Department of Energy, Nuclear Physics Division, under Contract No. W-31-109-ENG-38. The Department of Energy, High Energy Physics Division, supported the work of Harvard University, the Unversity of Maryland, the Massachussetts Institute of Technology under Contract No. DE-AC02-76ER03069, Northwestern University under Contract No. DE-FG02-91ER40684, and Yale University. The Albert-Ludwigs Universität and the University of Wuppertal were supported in part by the Bundesministerium für Forschung und Technologie.

[1] Current address: Alaskaweg 20, 2000 Hamburg 73, Germany.
[2] Current address: Lawrence Livermore National Laboratory, Livermore, CA 94550, USA.
[3] Current address: The Rockefeller University, New York NY 10021, USA.
[4] Current address: Loma Linda University Medical Center, Loma Linda CA 92350, USA.
[5] Current address: DESY, Notkestraße 85, 2000 Hamburg, Germany.
[6] Current address: Rutgers University, Piscataway, NJ 08855, USA.
[7] Current address: LeCroy Research Systems, Spring Valley, NY 10977, USA.
[8] Current address: Laboratoire de l'Accélérateur Linéaire, F-91405 Orsay, France.
[9] Current address: Los Alamos National Laboratory, Los Alamos, NM 87545, USA.
[10] Current address: Argonne National Laboratory, Argonne, IL 60439, USA.
[11] Current address: California Institute of Technology, Pasadena, CA 91125, USA.
[12] Current address: Oxford University, Oxford OX1 3RH, UK.
[13] Current address: Fermi National Accelerator Laboratory, Batavia, IL 60510, USA.
[14] Deceased.
[15] Current address: Universität Bochum, W-4630 Bochum, Germany.
[16] Current address: A. T. & T, Bell Labs, 2000 North Naperville Road, Naperville, IL, USA.
[17] Current address: University of Wisconsin, Madison, WI 53706, USA.
[18] Current address: Superconducting Super Collider Laboratory, Dallas, TX 75237, USA.
[19] Current address: Albert-Ludwigs-Universität, W-7800 Freiburg, Germany.
[20] Current address: Northern Illinois University, Dekalb, IL 60115, USA.
[21] Current address: Texas A&M Univ., College Station, TX 77843, USA.

References

[1] B. Badełek *et al.*, Rev. Mod. Phys. 64 (1992) 927.

[2] E.M. Levin, Nucleon structure function at small x, in: Proc. Joint International Lepton-Photon Symposium and Europhysics Conference on High-Energy Physics (Geneva, Switzerland, July 1991), Vol. 1, ed. S. Hegarty, K. Potter, E. Quercigh (World Scientific, Singapore, 1992) p. 170.

[3] B. Badełek and J. Kwieciński, Phys. Lett. B 295 (1992) 263.

[4] H. Abramowicz *et al.*, Phys. Lett. B 269 (1991) 465.

[5] P. Amaudruz *et al.*, Phys. Lett. B 295 (1992) 159;
I.G. Bird, Ph.D. Thesis, Free University, Amsterdam (1992), unpublished.

[6] P. Amaudruz *et al.*, Phys. Rev. Lett. 66 (1991) 2712;
P. Amaudruz *et al.*, Nucl. Phys. B 371 (1992) 3;
M.W. van der Heijden, Ph.D. Thesis, University of Amsterdam (1991), unpublished.

[7] D.O. Caldwell *et al.*, Phys. Rev. D 7 (1973) 1362.

[8] A.A. Bhatti, Ph.D. Thesis, University of Washington (1991), unpublished;
S. Aïd, Ph.D. Thesis, University of Maryland (1991), unpublished.

[9] L.W. Whitlow *et al.*, Phys. Lett. B250 (1990) 193.

[10] M.R. Adams *et al.*, Nucl. Instr. Methods A 291 (1990) 533.

[11] M.R. Adams *et al.*, Phys. Rev. Lett. 68 (1992) 3266.

[12] L.L. Frankfurt and M.I. Strikman, Phys. Lett. B 76 (1978) 333.

[13] A.C. Benvenuti *et al.*, Phys. Lett. B 237 (1990) 599.

[14] B. Badełek and J. Kwieciński, Nucl. Phys. B 370 (1992) 278.

[15] V.R. Zoller, Phys. Lett. B 279 (1992) 145.

[16] K. Gottfried, Phys. Rev. Lett. 18 (1967) 1174.